Enhanced groundwater recharge rates and altered recharge sensitivity to climate variability through subsurface heterogeneity

Andreas Hartmann[a,b,1], **Tom Gleeson**[c,d], **Yoshihide Wada**[e,f,g,h], **and Thorsten Wagener**[b,i]

[a]Institute of Earth and Environmental Sciences, University of Freiburg, Freiburg, Germany; [b]Department of Civil Engineering, University of Bristol, Bristol, United Kingdom; [c]Department of Civil Engineering, University of Victoria, Victoria, BC, Canada; [d]School of Earth and Ocean Sciences, University of Victoria, Victoria, BC, Canada; [e]International Institute for Applied Systems Analysis, A-2361 Laxenburg, Austria; [f]NASA Goddard Institute for Space Studies, New York, NY 10025; [g]Center for Climate Systems Research, Columbia University, New York, NY 10025; [h]Department of Physical Geography, Utrecht University, 3584 CS Utrecht, The Netherlands; and [i]Cabot Institute, University of Bristol, Bristol, United Kingdom

Edited by Dieter Gerten, Potsdam Institute for Climate Impact Research, Potsdam, Germany, and accepted by Editorial Board Member Hans J. Schellnhuber January 18, 2017 (received for review September 6, 2016)

Our environment is heterogeneous. In hydrological sciences, the heterogeneity of subsurface properties, such as hydraulic conductivities or porosities, exerts an important control on water balance. This notably includes groundwater recharge, which is an important variable for efficient and sustainable groundwater resources management. Current large-scale hydrological models do not adequately consider this subsurface heterogeneity. Here we show that regions with strong subsurface heterogeneity have enhanced present and future recharge rates due to a different sensitivity of recharge to climate variability compared with regions with homogeneous subsurface properties. Our study domain comprises the carbonate rock regions of Europe, Northern Africa, and the Middle East, which cover ∼25% of the total land area. We compare the simulations of two large-scale hydrological models, one of them accounting for subsurface heterogeneity. Carbonate rock regions strongly exhibit "karstification," which is known to produce particularly strong subsurface heterogeneity. Aquifers from these regions contribute up to half of the drinking water supply for some European countries. Our results suggest that water management for these regions cannot rely on most of the presently available projections of groundwater recharge because spatially variable storages and spatial concentration of recharge result in actual recharge rates that are up to four times larger for present conditions and changes up to five times larger for potential future conditions than previously estimated. These differences in recharge rates for strongly heterogeneous regions suggest a need for groundwater management strategies that are adapted to the fast transit of water from the surface to the aquifers.

groundwater recharge | subsurface heterogeneity | water resources | climate variability | climate change

Groundwater recharge is a crucial component of the global water balance, feeding the world's groundwater storages and thereby supplying fresh water to large parts of the global population (1–4). Comparing groundwater recharge with groundwater use and ecological water demand helps to distinguish between overused aquifer systems and aquifer systems that still allow for more abstraction in a sustainable way (5, 6). The importance of managing groundwater sustainably will increase in the future given the growing dependence on this resource in many parts of the world (7). Subsurface heterogeneity notably affects groundwater recharge (4), especially in weathered carbonate rock regions (8). Spatially variable soil thickness and hydraulic conductivity in the subsurface produce fast, localized vertical water movement, thereby enhancing groundwater recharge (9). Our study takes into account the impact of subsurface heterogeneity on present and potential future recharge rates at a continental scale. Subsurface heterogeneity evolves for various reasons (10). In this paper, we confine our modeling domain to carbonate rock regions. Such regions typically exhibit the most extreme subsurface heterogeneity in terms of hydraulic conductivities and storage capacities due to the weathering of carbonate rock, a process also referred to as "karstification" (11, 12). We focus on Europe, Northern Africa, and the Middle East, where ∼560 million people depend on drinking water from karst aquifers (13, 14) and where information on karst recharge is most available.

We simulate groundwater recharge (defined here as the simulated vertical downward flux entering the saturated zone) using both a homogeneous and a heterogeneous subsurface representation (Fig. 1). The global hydrological model PCR-GLOBWB (15) is used for the homogeneous subsurface representation, whereas the karst recharge model VarKarst-R (16), which includes variable thickness of the soil, epikarst (the weathered interface of soil and carbonate rock), and hydraulic conductivity, is used for the heterogeneous representation. The structure of VarKarst-R is particularly adapted to the dominant hydrological processes of carbonate regions allowing for focused preferential recharge and variable subsurface dynamics that are found in humid, Mediterranean, mountainous, and desert karst regions (16). These processes are not included in the PCR-GLOBWB model or

ENVIRONMENTAL SCIENCES

SUSTAINABILITY SCIENCE

Significance

Understanding the implications of climate changes on hydrology is crucial for water resources management. Widely used global hydrological models generally assume simple homogeneous subsurface representations to translate climate signals into hydrological variables. We study groundwater recharge in the carbonate rock regions of Europe, Northern Africa, and the Middle East, which are known to exhibit strong subsurface heterogeneity. We demonstrate that subsurface heterogeneity alters the sensitivity of recharge to climate variability and enhances recharge estimates, resulting in potentially more available water per capita, than previously estimated. Our results are opposing previous modeling studies on future groundwater availability that assumed homogeneous subsurface properties everywhere. We suggest that water management strategies in regions with heterogeneous subsurface properties need to consider these revised estimates.

Author contributions: A.H., T.G., Y.W., and T.W. designed research; A.H. performed research; A.H., T.G., Y.W., and T.W. analyzed data; Y.W. provided the simulations of the PCR-GLOBWB model; and A.H. wrote the paper.

The authors declare no conflict of interest.

This article is a PNAS Direct Submission. D.G. is a Guest Editor invited by the Editorial Board.

[1]To whom correspondence should be addressed. Email: andreas.hartmann@hydrology.uni-freiburg.de.

This article contains supporting information online at www.pnas.org/lookup/suppl/doi:10.1073/pnas.1614941114/-/DCSupplemental.

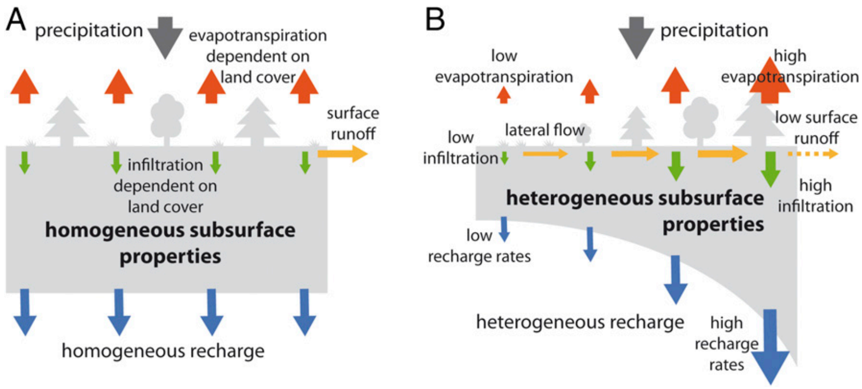

Fig. 1. Homogeneous and heterogeneous representations of the subsurface. Two different representations of the subsurface of a simulation grid-cell (0.5 × 0.5°): (*A*) homogeneous subsurface representation by the PCR-GLOBWB global simulation model (15) and (*B*) heterogeneous subsurface representation by the VarKarst-R large-scale karst recharge model (16).

other comparable large-scale hydrological models. We use the output of five general circulation models [GCMs of the ISI-MIP model ensemble (17), 0.5 × 0.5° resolution] to simulate groundwater recharge with each of these two subsurface representations, from 1991 to 2099 under the highest emission scenario [RCP8.5 (18), increasing radiative forcing, >8.5 Wm^{-2} by 2100, and increasing atmospheric CO_2 concentrations, >1,370 ppm. CO_2-equivalent by 2100). To avoid biasing our results by selecting one specific GCM, we use ensemble means for all our interpretations after applying all five GCMs individually to both subsurface representations, respectively.

We assess recharge sensitivity to climate variability using the statistical elasticity measure. Beyond a correlation analysis that simply evaluates the strength of relations between variables, elasticity quantifies "how responsive one variable is to change in another variable" (19) or "the percentage change in a first variable to the percentage change in second variable, when the second variable has a causal influence on the first variable" (20). Among several applications of elasticity on stream flow (21–23), we apply elasticity to groundwater recharge in hydrology. Here we define recharge sensitivity as the median ratio of interannual changes of recharge rates to the interannual changes of three climatic variables that drive recharge and evapotranspiration using a 20-y period: (*i*) Annual precipitation expresses general water availability, (*ii*) mean annual temperature is used as proxy for potential evapotranspiration, and (*iii*) the mean intensity of high-intensity events is used to account for the nonlinear impact of strong rainfall events (24). Similar to ref. 23, we preferred temperature over net radiation as a proxy for potential evapotranspiration because net radiation is temperature dependent and temperature is the best-understood and most common input variable to large-scale hydrological models. Recharge sensitivity with large positive or negative values indicates that recharge is highly sensitive to variations of these input variables. Values closer to 0 indicate a low sensitivity. Recharge sensitivity to precipitation and to high-intensity events is calculated with changes normalized by their 20-y average ($\%\%^{-1}$), whereas recharge sensitivity to temperature is expressed by normalized changes of recharge per absolute change of temperature ($\%\,°C^{-1}$). Further elaborations on the simulation models, the input variables, and the recharge elasticity are provided in *Materials and Methods*.

Realism of Heterogeneity Processes

A comparison with observations indicates that the heterogeneous model provides more realistic simulations of recharge than the homogeneous model because it includes heterogeneity processes. For validation we compare the recharge simulations of the two models driven by the 5 climate models for the present period (1991–2010) with independent recharge observations for 38 karst systems in Europe for which we could obtain recharge values from the literature (ref. 16 and Table S1). To better understand how much subsurface heterogeneity is actually responsible for the differences of recharge estimations of the two models, we additionally compare the observations from our literature review with simulations of a version of the heterogeneous model where the heterogeneity processes are turned off (i.e., homogeneous subsurface, no lateral flow concentration but surface runoff leaves the grid cell). We find that, although significant remains, the simulations of the heterogeneous model plot around the 1:1 line (average deviation 55.8 mma^{-1}, Fig. 2), whereas most of the homogeneous models simulations tend to

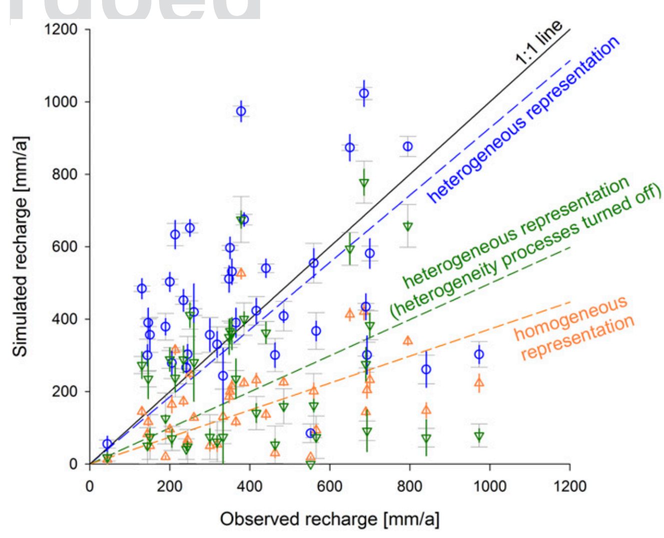

Fig. 2. Comparison of simulations and observations. Simulated recharge volumes of the heterogeneous model (VarKarst-R), the homogeneous model (PCR-GLOBWB), and the heterogeneous model with subsurface heterogeneity processes turned off plotted against observed recharge volumes (Table S1); colored and gray whiskers indicate the simulation uncertainty (1 SD) due to the five climate models and due to parameter uncertainty (only heterogeneous model and heterogeneous model with heterogeneity processes turned off; *Materials and Methods*), respectively. We find a significant difference ($P < p < 10^{-5}$) between the heterogeneous model and the homogeneous model, as well as between the heterogeneous model and the heterogeneous model with heterogeneity processes turned off. There is no statistical difference (5% significance level) between the homogeneous model and the heterogeneous model with heterogeneity processes turned off, as well as between the heterogeneous model and the observations.

underestimate recharge (average deviation −232.9 mma^{-1}, Fig. 2). When we turn off the heterogeneity processes of the heterogeneous model, its simulations also fall in large parts below the 1:1 line, plotting closer to the simulations of the homogeneous model (average deviation −167.4 mma^{-1}). These results do not mean that subsurface heterogeneity is the only reason for the different simulated recharge rates of the heterogeneous and homogeneous subsurface representations, because the models also differ with respect to other processes, such as interception or capillary rise of groundwater (*Materials and Methods*). However, our comparison suggests that disregarding heterogeneity processes can result in an overall underestimation of recharge, at least for the 38 karst systems that we used in our evaluation.

Recharge Sensitivity to Climate Variability

We further find that the two subsurface representations exhibit different sensitivities to climate variability. We divide all carbonate rock areas into four regions defined by cluster analysis using climatic and topographic descriptors (16) (Fig. 4): humid (HUM), mountains (MTN), Mediterranean (MED), and deserts (DES). Q:21 Recharge sensitivities to climate variability are calculated for the time period of 1991–2010. Between the four regions, we find a mixed pattern of sensitivity values (Fig. 3 and Fig. S1). We can see that recharge sensitivities to rainfall change from high to low values when moving from wet (humid) to dry (desert) regions for both model representations. The Mediterranean and desert regions mostly exhibit a higher sensitivity to climate variability. The same gradient from wet to dry is found for high-intensity events. We observe the opposite trend for recharge sensitivity to temperature, which increases from humid toward the Mediterranean regions but decreases again in the desert.

For the Mediterranean and desert regions, the heterogeneous representation shows higher sensitivity to changes in annual precipitation, mean annual temperature, and high-intensity rainfall events. Recharge estimates of the homogeneous model tend to be more sensitive to changes in precipitation in the humid and mountain regions, as well as to changes in high-intensity rainfall events in the mountain regions. Sensitivities to temperature changes in the humid and mountain regions and to high-intensity rainfall events in the humid regions are similar for both subsurface representations. The general pattern of recharge sensitivities can be explained through the increased fractions of precipitation that become evapotranspiration (25, 26) when moving from the humid toward the desert regions. Water availability (precipitation) is the most important control on recharge sensitivities in the humid region, whereas temperature is the stronger control in the Mediterranean regions. In the desert region, recharge sensitivity generally decreases, as there is simply little water available for evapotranspiration.

The different recharge sensitivities with respect to climate variability for the two subsurface representations can be explained by the interplay of two different simulated processes: (*i*) variable fractions of surface runoff, which dynamically increase or reduce infiltration, and (*ii*) different dynamics of evapotranspiration that change the amount of water available for downward percolation. The first explains the higher sensitivities of the homogeneous subsurface representation to humid and mountain region precipitation. The homogeneous model calculates fractions of surface runoff with a nonlinear relationship to wetness that is more sensitive for the wet conditions prevailing in humid and mountain regions (Eq. **1**, *Materials and Methods*). The same process explains the higher sensitivity of the homogeneous model to high-intensity rainfall events. No such partitioning takes place for the heterogeneous model, which produces focused recharge instead of surface runoff and therefore is less sensitive to changes in precipitation and high-intensity rainfall events in those wet regions (humid, mountain). On the other hand, the explicit calculation of soil storages with variable storage capacities in the heterogeneous subsurface representation (Fig. 1*B* and Eq. **2**, *Materials and Methods*) results in different evapotranspiration dynamics than found in the homogeneous model. Whereas soil compartments with small storage capacities saturate rapidly and produce focused recharge even during small and moderate rainfall events, the uniform soil storages of the homogeneous model (Fig. 1*A*) remain unsaturated more often and produce more evapotranspiration. This stronger pronunciation of evapotranspiration in the homogeneous model is the reason why its simulated recharge is less sensitive to all three input variables for the Mediterranean and the desert regions.

Future Groundwater Recharge

The differences in recharge sensitivity to variability in climate result in different simulated present and future recharge rates over Europe's carbonate rock regions. Compared with the homogeneous subsurface representation, the heterogeneous subsurface representation shows enhanced and more variable recharge rates for both present and future conditions (Fig. 4 and Fig. S3). In the present period (1991–2010), the simulated re- Q:22 charge rates of the heterogeneous subsurface representation are 2.1–4.3× larger than the recharge rates of the homogeneous representation. Toward the end of the century (2080–2099), the five GCMs indicate that in the humid region, future annual precipitation will remain more or less the same (2% of absolute increase), whereas considerable decreases are projected for the mountain (−14%), Mediterranean (−19%), and desert regions (−12%). Temperatures are predicted to increase for all regions, by 2.0, 4.9, 5.2, and 8.1 °C in the humid, mountain, Mediterranean, and desert regions, respectively. Future mean intensity of high-rainfall events is predicted to increase for the humid (11%),

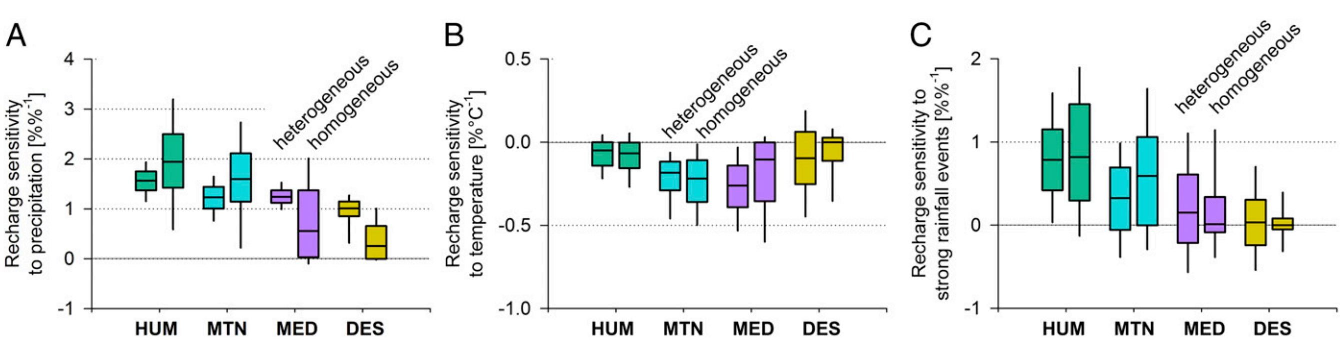

Fig. 3. Sensitivity to climate variability. Recharge sensitivity to (*A*) annual precipitation, (*B*) mean annual temperature, and (*C*) high-intensity events (mean intensity of the upper quartile of rainfall events) for the four regions (HUM, MTN, MED, and DES) at the present (1991–2010); uncertainty of simulated recharge sensitivities of the heterogeneous model due to parameter uncertainty (*Materials and Methods*) to annual precipitant, temperature, and strong rainfall events varies by 0.13–0.24$\%\%^{-1}$, 0.03–0.18$\%°C^{-1}$, and 0.18–0.37$\%\%^{-1}$, respectively (1 SD, increasing from humid to desert regions).

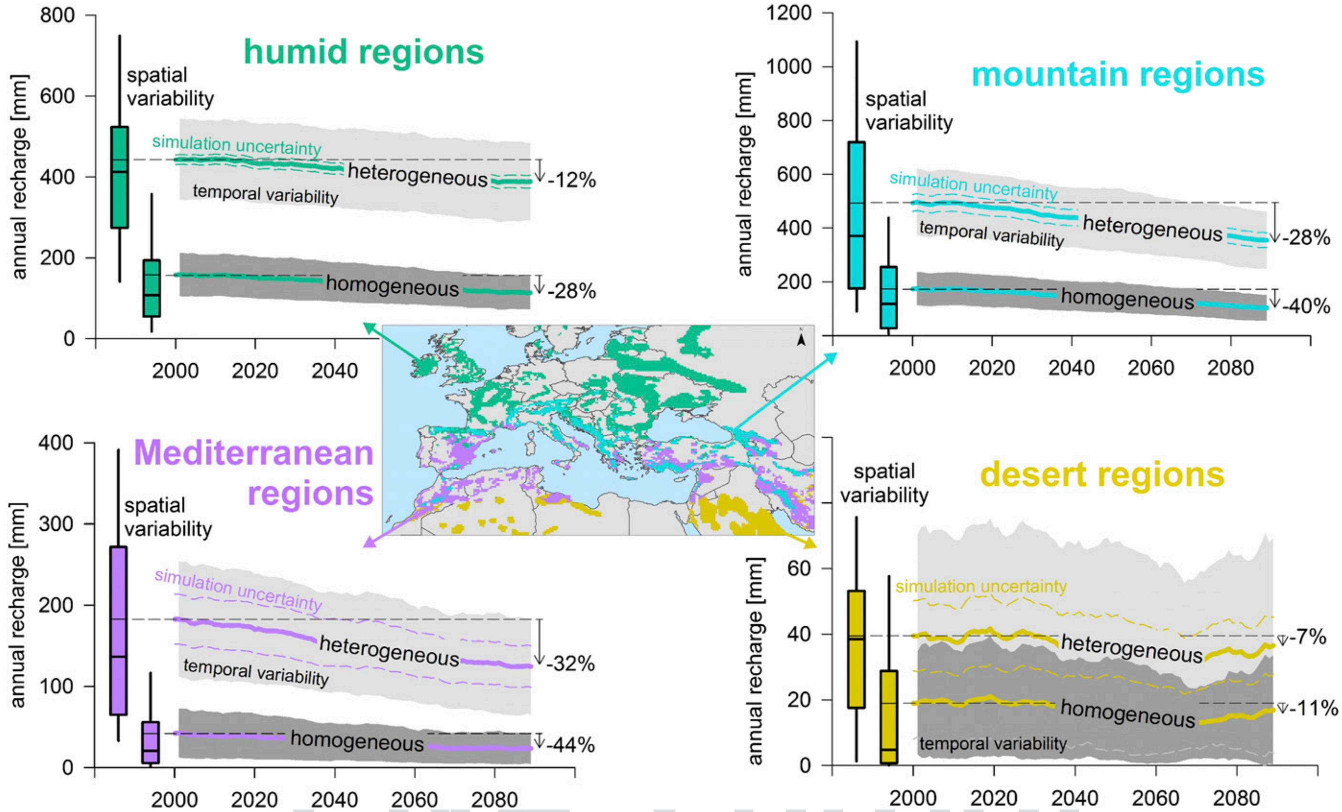

Fig. 4. Simulation of future groundwater recharge. Simulation results for the two subsurface representations for four regions; spatial variability within each region for the present (1991–2010) is presented by the boxplots; temporal evolution of recharge rates is expressed by a 20-y moving average (centered around its mean year, for instance the year 2000 for the 1991–2010 average); temporal variability within each 20-y window is expressed by its SD indicated by the gray shading around the mean (gray dashed line represents lower boundary of the heterogeneous model temporal variability at the desert regions); simulation uncertainty of the heterogeneous model due to parameter uncertainty (*Materials and Methods*) is indicated by the dashed lines around the mean recharge.

mountain (8%), and Mediterranean (7%) regions, whereas there is no trend for the desert region (1% increase) (Fig. S2).

As a result of the projected climatic change, we find a general reduction of recharge rates for both subsurface representations, which is consistent with previous findings on the changes of future stream flow during low-flow conditions (27). The relative decrease of the two subsurface representations is in the same direction. We find reductions of 7–32 and 11–44% for the heterogeneous and the homogeneous representations, respectively (Fig. 4 and Fig. S3). However, the absolute reductions of simulated recharge rates of the heterogeneous representation (3–138 mma^{-1}) are 2.2–5.3× larger than the simulated reductions of the homogeneous representation (2–79 mma^{-1}). Interannual variability of recharge is also becoming more pronounced for the heterogeneous representation. This variability increases from the humid and mountain regions to the deserts, likely due to the increased variability of rainfall events in dry regions (28). In particular, convective storm events are known to produce large fractions of preferential recharge in semiarid or arid regions (9). Whereas recharge rates of both simulations are predicted to decrease in all regions, temporal variability within the 20-y averages does not change significantly over the same time horizon. Hence, with a general decrease of recharge rates, the interannual variability of groundwater recharge in heterogeneous regions will gain more importance, especially in the Mediterranean, where we expect an increase in impact of high-intensity events.

Discussion

Focused recharge is known to be an important process of recharge generation in regions with heterogeneous subsurface characteristics (4, 29) and its strong impact on overall groundwater recharge amounts has been shown in several studies at the catchment scale (30–32). Our recharge sensitivity analysis reveals that accounting for this process and the variability of soil storages at a much larger spatial scale results in different recharge sensitivities compared with a homogeneous subsurface representation that does not consider focused recharge. We demonstrate that a heterogeneous recharge modeling approach is more consistent with independent recharge estimates of other studies for karst regions, and therefore more likely to be a reasonable representation of the water balance separation occurring across the study region than current modeling approaches. Our subsequent findings indicate that the water balance of heterogeneous areas in the Mediterranean and desert regions will be less dominated by evapotranspiration compared with regions with homogeneous subsurface properties because water is rapidly passed downward. The heterogeneous subsurface representation also suggests smaller amounts of surface runoff than the homogeneous representation. On the other hand, the presence of focused recharge and variable soil storage capacities generally results in higher recharge rates, which are less affected by the variability of precipitation and high-intensity events in the humid and mountain regions.

Hence, due to the presence of heterogeneity processes, a greater proportion of the water cycle is active in the subsurface, meaning the risk of overexploitation may be lower than previously considered. Dividing the difference of recharge simulations of the heterogeneous model and mean recharge simulations of the homogeneous model in the four regions by their population (Fig. S4) indicates that an additional ∼1,000–3,300 m^3 of groundwater per capita per year are potentially available at the present (2,900, 3,300, 1,500, and 950 m^3 per capita per year for the humid, mountain, Mediterranean, and desert region, respectively). Especially in the Mediterranean, where previous modeling studies expect significant groundwater stress (5), the additional future recharge of 1,000 m^3 of groundwater per capita per year may potentially lead to less future groundwater stress than previously expected.

However, estimated groundwater recharge volumes do not equal exploitable groundwater fluxes because a number of factors can limit the use of this simulated surplus recharge. First, groundwater pumping likely decreases groundwater discharge significantly, with spring flow and base flow impacting environmental flow (1, 33). Q:24 Second, groundwater recharge in carbonate rock aquifers may quickly leave the aquifer through large conduit systems and springs (8). Third, recharge that is stored within the aquifer may not be fully available for development as abstraction wells are usually unable to access the entire volume of the aquifer (33). Fourth, the high temporal variability of recharge in heterogeneous regions, which is most pronounced at the Mediterranean and desert regions (Fig. 4), may prohibit continuous withdrawal of groundwater. Finally, higher recharge rates imply an increased vulnerability to surface contamination due to preferential recharge, which might reduce the value of the groundwater resource (34).

Possible water management strategies include adapted water management plans that take into account the variable flow dynamics of these aquifers with heterogeneous recharge behavior. For instance, groundwater-pumping rates could be adapted to the temporally variable water availability (35). Additionally, temporal variability could be compensated for by artificially recharging aquifers with longer residence times using water discharged from the more heterogeneous regions (36, 37). Regardless, the requirements to sustain environmental flow (1) and the increased vulnerability to contamination due to preferential recharge (34) have to be accounted for in any water management plan. The concerns are especially acute in the Mediterranean region, where the expected increase of rainfall intensity and the high interannual variability of recharge will require adapted measures for water resources management and protection to finally use the potentially additional recharge that we found in our study. Such management strategies are important because 116 million inhabitants and 80% of agriculture depend on irrigation (Fig. S4) in the Mediterranean region.

This study focuses on how to represent subsurface heterogeneity in large-scale hydrological models. Our results imply that subsurface heterogeneity significantly alters groundwater recharge and its sensitivity to climate variability at large spatial scales. The explicit consideration of variable storage capacities and focused recharge within the heterogeneous model is compared Q:25 with previous large-scale modeling studies that considered their soil layers to be homogeneous (38, 39). Considering heterogeneity processes within our model produces less evapotranspiration and surface runoff and more groundwater recharge. This difference produces potentially more available groundwater per capita than previously estimated (15). Current simulations of land surface–atmosphere coupling (26), drought occurrence (27, 40), flood frequency projections (41), or water scarcity assessment (42) are currently based on large-scale hydrological models with homogeneous subsurface representations. Our study shows that their results may have reduced utility for groundwater management for regions with pronounced subsurface heterogeneity. Through our parsimonious simulation approach, we also provide a promising direction to include subsurface heterogeneity evolved due to karstification into any large-scale hydrological model to obtain more realistic simulations.

Materials and Methods

The Homogeneous Model: PCR-GLOBWB. The PCR-GLOBWB model (15) simulates the terrestrial water balance on a 0.5 × 0.5° grid using a daily temporal resolution. Soil water balance of two homogeneous soil layers and a single underlying aquifer layer is calculated at each time step. Simulated hydrological processes comprise infiltration of rainfall and snowmelt, evapotranspiration, interception, downward percolation from the upper soil layer to the lower soil layer and from the lower soil layer to the aquifer layer (which is the flux we consider the simulated recharge of the homogeneous model in this study), and capillary rise from the groundwater up to the unsaturated soil. The model parameters are found using prior information from public sources, e.g., the FAO Digital Soil Map of the World (43) or a simplified version of the litho- Q:26 logical map of the world (44). No calibration is performed.

Like other global hydrological models (38, 45), PCR-GLOBWB uses a distribution function to account for the impact of spatial variability of land-surface properties on the generation of surface runoff:

$$x(t) = 1 - \left(\frac{S(t)}{S_{\max}}\right)^{b/(b+1)}, \qquad [1]$$

where $x(t)$ is the fraction of effective precipitation at time t that becomes surface runoff, $S(t)$ is the total soil storage (layers 1+2) at time t, S_{max} is the maximum total soil storage, and b is a dimensionless shape factor based on subgrid information on the distribution of land-cover classes with tall and short vegetation, paddy and nonpaddy irrigation, land and open water, and different soil types (46). The surface runoff calculated by Eq. **1** leaves the grid cell toward the stream (Fig. 1*A* in the research letter). Q:27

The Heterogeneous Model, VarKarst-R. The VarKarst-R(16) also simulates terrestrial hydrological processes on a 0.5 × 0.5° grid and at a daily temporal resolution. Its structure considers infiltration of rainfall and snowmelt, evapotranspiration, downward percolation from the upper soil layer to a lower soil epikarst layer, and vertical percolation from the epikarst layer toward the groundwater (which is the flux we defined as simulated recharge of the heterogeneous model in this study). The epikarst in the second layer is a typical feature of karst systems regarded as the hydrological unit that controls the dynamic separation of focused and diffuse groundwater recharge (47, 48). In general, the VarKarst-R model has a simpler structure (only 4 free parameters) compared with PCR-GLOBWB (29 free parameters) as it uses fewer explicit representations of hydrological processes, for instance it does not explicitly consider interception or capillary rise from the groundwater.

The special feature of the VarKarst-R model is its assumption that even within the same hydrological landscape type there is a distribution of subsurface properties. This variability is expressed by distribution functions that allow for variability of soil and epikarst storage capacities, as well as of epikarst hydraulic properties, over N horizontally parallel model compartments (Fig. 1*B*):

$$S_{\max,i} = S_{\max,N}\left(\frac{i}{N}\right)^{a}, \qquad [2]$$

$$K_{epi,i} = K_{epi,1}\left(\frac{N-i+1}{N}\right)^{a}, \qquad [3]$$

where $S_{max,i}$ (mm) is the soil or epikarst storage capacity of model com- Q:28 partment i, $S_{max,N}$ (mm) is the overall maximum storage capacity of the soil or the epikarst, $K_{epi,i}$ [d] is the storage constant of the epikarst at model compartment i, $K_{epi,1}$ [d] is the storage constant of the epikarst at model compartment 1, and a [–] is a dimensionless shape factor. Using the distributions from Eqs. **2** and **3**, soil and epikarst water balance are simultaneously calculated at each time step and in each model compartment. The epikarst can only reach saturation when infiltration exceeds vertical percolation (actual epikarst storage divided by $K_{epi,i}$).The fraction of effective precipitation that exceeds soil and epikarst water deficit becomes surface runoff. However, in contrast to PCR-GLOBWB, surface runoff is not routed toward the streams but transferred laterally to the next model compartment (from i to i+1) where it is added again to effective precipitation. Increasing epikarst permeability (Eq. **3**), therefore, allows for lateral flow concentration along the model compartments (Fig. 1*B* in the research letter). Q:29

Because large-scale information on subsurface heterogeneity in carbonate rock regions is not available, a procedure to estimate the VarKarst-R model Q:30 parameters was developed (16). Based on cluster analysis and the concept of hydrological landscapes that includes climate and topographic information (16, 49), carbonate rock regions are divided into four regions: humid (HUM), mountains (MTN), Mediterranean (MED), and deserts (DES). A large sample of initial model parameter sets (n = 25,000) is iteratively reduced using prior information [e.g., the FAO Digital Soil Map of the World (43)], FLUXNET (50) Q:31 latent heat flux observations, and soil moisture observations of the International Soil Moisture Network (51) in each of the regions. For each karst landscape, the reduced parameters ranges of acceptable latent heat flux and soil moisture simulations directly express the remaining parameter uncertainty. For this study, we sampled 250 parameter sets from these reduced ranges to obtain an ensemble of 250 model realizations in each grid cell to quantify the uncertainty of the VarKarst-R recharge simulations due to the parameter estimation process.

Climate Change Scenarios. Both simulation models are driven by the same climate forcing derived from the bias-corrected five GCMs of the ISI-MIP data (17). We chose the highest emission scenario of available Representative Concentrations Pathways (RCP 8.5), with strongly increased radiative forcing and atmospheric CO_2 concentrations (18) to obtain the worst-case scenario between current and future conditions. Similar to previous studies on climate change impacts (26), we consider 20-y periods to analyze changes in climate and groundwater recharge. By calculating running averages and their SD of the GCM ensemble mean for each of the four subregions, we can assess average recharge and its sensitivity to climate variability, including their transitions toward the end of this century.

Elasticity Calculations. We define recharge elasticity E_R [–] as the median of the interannual changes of recharge rates R (mma^{-1}) according to transannual changes of a controlling variable X, normalized by their annual means over a predefined period (e.g., 20 y):

$$E_R = median\left(\frac{\Delta R}{\Delta X}\right). \quad [4]$$

As in previous studies (19, 21), we prefer the median of transannual changes Q:32
rather than their mean to avoid bias due to outliers. As control variables, we consider annual precipitation P (mm), temperature T (°C), and the annual mean of rainfall intensity of high-intensity events H_{INT} (mm·d^{-1}), defined as the mean intensity of the upper quartile of rainfall events. Hereby P represents the influence of the total annual water availability on recharge, T is a proxy for the influence of energy available for evapotranspiration, and H_{INT} is an indicator for the influence of strong rainfall events on recharge (also see elaborations in the letter above). Similar to other studies (26), we consider 20 y long enough to reflect climatic variability. Whereas R, P, and H_{INT} are normalized by their mean over this 20-y period, we do not normalize T because temperature changes cannot be meaningfully represented as percent.

ACKNOWLEDGMENTS. This work was supported by a fellowship to A.H. within the Postdoc Programme of the German Academic Exchange Service.

1. Gleeson T, Wada Y, Bierkens MF, van Beek LP (2012) Water balance of global aquifers revealed by groundwater footprint. *Nature* 488(7410):197–200.
2. Taylor RG, et al. (2012) Ground water and climate change. *Nat Clim Chang* 3(4): 322–329.
3. Döll P, Fiedler K (2008) Global-scale modeling of groundwater recharge. *Hydrol Earth Syst Sci* 12(3):863–885.
4. de Vries JJ, Simmers I (2002) Groundwater recharge: An overview of processes and challenges. *Hydrogeol J* 10(1):5–17.
5. Wada Y, Van Beek LPH, Bierkens MFP (2012) Nonsustainable groundwater sustaining irrigation: A global assessment. *Water Resour Res* 48(1), 10.1029/2011WR010562.
6. Aeschbach-Hertig W, Gleeson T (2012) Regional strategies for the accelerating global problem of groundwater depletion. *Nat Geosci* 5(12):853–861.
7. Gleeson T, et al. (2010) Groundwater sustainability strategies. *Nat Geosci* 3(6): 378–379. Q:33
8. Ford DC, Williams PW (2013) *Karst Hydrogeology and Geomorphology* (John Wiley & Sons, Chichester, UK). Q:34
9. Scanlon BR, et al. (2006) Global synthesis of groundwater recharge in semiarid and arid regions. *Hydrol Processes* 20(15):3335–3370.
10. McDonnell JJ, et al. (2007) Moving beyond heterogeneity and process complexity: A new vision for watershed hydrology. *Water Resour Res* 43(7):W07301.
11. Ford DC, Williams PW (2007) *Karst Hydrogeology and Geomorphology* (Wiley, Chichester, UK). Q:35
12. Worthington SRH, Davies GJ, Alexander EC (2016) Enhancement of bedrock permeability by weathering. *Earth Sci Rev* 160:188–202.
13. Hartmann A, Goldscheider N, Wagener T, Lange J, Weiler M (2014) Karst water resources in a changing world: Review of hydrological modeling approaches. *Rev Geophys* 52(3):218–242.
14. COST (1995) COST 65: Hydrogeological aspects of groundwater protection in karstic areas, Final Report (COST action 65). *Eur Comm Dir XII Sci Res Dev* Report EUR:446. Q:36
15. Wada Y, Wisser D, Bierkens MFP (2014) Global modeling of withdrawal, allocation and consumptive use of surface water and groundwater resources. *Earth Syst Dyn* 5(1):15–40.
16. Hartmann A, et al. (2015) A large-scale simulation model to assess karstic groundwater recharge over Europe and the Mediterranean. *Geosci Model Dev* 8(6):1729–1746.
17. Hempel S, Frieler K, Warszawski L, Schewe J, Piontek F (2013) A trend-preserving bias correction – the ISI-MIP approach. *Earth Syst Dyn* 4(2):219–236.
18. Moss RH, et al. (2010) The next generation of scenarios for climate change research and assessment. *Nature* 463(7282):747–756.
19. Schaake JC (1990) From climate to flow. *Climate Change and US Water Resources*, ed Waggoner PE (John Wiley, New York), pp 177–206.
20. OECD (1993) *Glossary of Industrial Organisation Economics and Competition Law*, eds Khemani RS, Shapiro DM (Organisation for Economic Co-operation and Development, commissioned by the Directorate for Financial, Fiscal and Enterprise Affairs, [redacted]). Q:37
21. Andréassian V, Coron L, Lerat J, Le Moine N (2015) Climate elasticity of streamflow revisited – an elasticity index based on long-term hydrometeorological records. *Hydrol Earth Syst Sci Discuss* 12(4):3645–3679.
22. Berghuijs WR, Hartmann A, Woods RA (2016) Streamflow sensitivity to water storage changes across Europe. *Geophys Res Lett*, 10.1002/2016GL067927.
23. Vano JA, Das T, Lettenmaier DP (2012) Hydrologic sensitivities of Colorado River runoff to changes in precipitation and temperature. *J Hydrometeorol* 13(3):932–949. Q:38
24. Taylor RG, et al. (2012) Evidence of the dependence of groundwater resources on extreme rainfall in East Africa. *Nat Clim Chang* 3(4):374–378.
25. Prudhomme C, et al. (2014) Hydrological droughts in the 21st century, hotspots and uncertainties from a global multimodel ensemble experiment. *Proc Natl Acad Sci USA* 111(9):3262–3267.
26. Seneviratne SI, Lüthi D, Litschi M, Schär C (2006) Land-atmosphere coupling and climate change in Europe. *Nature* 443(7108):205–209.
27. Forzieri G, et al. (2014) Ensemble projections of future streamflow droughts in Europe. *Hydrol Earth Syst Sci* 18(1):85–108.
28. Lionello P (2012) *The Climate of the Mediterranean Region: From the Past to the Future* (Elsevier, [redacted]), 1st Ed. Q:39
29. Scanlon B, Healy R, Cook P (2002) Choosing appropriate techniques for quantifying groundwater recharge. *Hydrogeol J* 10(1):18–39.
30. Malard A, Sinreich M, Jeannin P (2015) A novel approach for estimating karst groundwater recharge in mountainous regions and its application. *Hydrol Process*, 10.1002/hyp.10765.
31. Andreo B, et al. (2008) Methodology for groundwater recharge assessment in carbonate aquifers: Application to pilot sites in southern Spain. *Hydrogeol J* 16(5):911–925.
32. Allocca V, Manna F, De Vita P (2014) Estimating annual groundwater recharge coefficient for karst aquifers of the southern Apennines (Italy). *Hydrol Earth Syst Sci* 18(2):803–817.
33. Bredehoeft JD (2002) The water budget myth revisited: Why hydrogeologists model. *Ground Water* 40(4):340–345.
34. Andreo B, et al. (2006) Karst groundwater protection: First application of a Pan-European Approach to vulnerability, hazard and risk mapping in the Sierra de Líbar (Southern Spain). *Sci Total Environ* 357(1-3):54–73.
35. Fleury P, Ladouche B, Conroux Y, Jourde H, Dörfliger N (2009) Modelling the hydrologic functions of a karst aquifer under active water management - The Lez spring. *J Hydrol (Amst)* 365(3–4):235–243.
36. Xanke J, Jourde H, Liesch T, Goldscheider N (2016) Numerical long-term assessment of managed aquifer recharge from a reservoir into a karst aquifer in Jordan. *J Hydrol (Amst)* 540:603–614.
37. Valhondo C, et al. (2016) Tracer test modeling for local scale residence time distribution characterization in an artificial recharge site. *Hydrol Earth Syst Sci Discuss* [redacted]:1–17. Q:40
38. Sood A, Smakhtin V (2015) Global hydrological models: A review. *Hydrol Sci J* 60(4): 549–565.
39. Davie JCS, et al. (2013) Comparing projections of future changes in runoff from hydrological and biome models in ISI-MIP. *Earth Syst Dyn* 4(2):359–374.
40. Dai A (2012) Increasing drought under global warming in observations and models. *Nat Clim Chang* 3(1):52–58.
41. Hirabayashi Y, et al. (2013) Global flood risk under climate change. *Nat Clim Chang* 3(9):816–821.
42. Schewe J, et al. (2014) Multimodel assessment of water scarcity under climate change. *Proc Natl Acad Sci USA* 111(9):3245–3250.
43. FAO (2003) *Digital Soil Map of the World* ([redacted], Rome). Q:41
44. Dürr HH, Meybeck M, Dürr SH (2005) Lithologic composition of the Earth's continental surfaces derived from a new digital map emphasizing riverine material transfer. *Global Biogeochem Cycles* 19(4):1–23.
45. Döll P, Kaspar F, Lehner B (2003) A global hydrological model for deriving water availability indicators: Model tuning and validation. *J Hydrol (Amst)* 270(1–2):105–134.
46. Hagemann S, Gates LD (2003) Improving a subgrid runoff parameterization scheme for climate models by the use of high resolution data derived from satellite observations. *Clim Dyn* 21(3–4):349–359.
47. Hartmann A, Lange J, Weiler M, Arbel Y, Greenbaum N (2012) A new approach to model the spatial and temporal variability of recharge to karst aquifers. *Hydrol Earth Syst Sci* 16(7):2219–2231.
48. Williams PW (1983) The role of the subcutaneous zone in karst hydrology. *J Hydrol (Amst)* 61:45–67.
49. Winter TC (2001) The concept of hydrologic landscapes. *JAWRA J Am Water Resour Assoc* 37(2):335–349.
50. Baldocchi D, et al. (2001) FLUXNET: A new tool to study the temporal and spatial variability of ecosystem–scale carbon dioxide, water vapor, and energy flux densities. *Bull Am Meteorol Soc* 82(11):2415–2434.
51. Dorigo WA, et al. (2011) The International Soil Moisture Network: A data hosting facility for global in situ soil moisture measurements. *Hydrol Earth Syst Sci* 15(5):1675–1698.

AUTHOR QUERIES

AUTHOR PLEASE ANSWER ALL QUERIES 1

Q: 1_Please contact PNAS_Specialist.djs@sheridan.com if you have questions about the editorial changes, this list of queries, or the figures in your article. Please include your manuscript number in the subject line of all email correspondence; your manuscript number is 201614941.

Q: 2_Please (i) review the author affiliation and footnote symbols carefully, (ii) check the order of the author names, and (iii) check the spelling of all author names, initials, and affiliations. Please check with your coauthors about how they want their names and affiliations to appear. To confirm that the author and affiliation lines are correct, add the comment "OK" next to the author line. This is your final opportunity to correct any errors prior to publication. Misspelled names or missing initials will affect an author's searchability. Once a manuscript publishes online, any corrections (if approved) will require publishing an erratum; there is a processing fee for approved erratum.

Q: 3_Please review and confirm your approval of the short title: Enhanced recharge through subsurface heterogeneity. If you wish to make further changes, please adhere to the 50-character limit. (NOTE: The short title is used only for the mobile app and the RSS feed.)

Q: 4_Please review the information in the author contribution footnote carefully. Please make sure that the information is correct and that the correct author initials are listed. Note that the order of author initials matches the order of the author line per journal style. You may add contributions to the list in the footnote; however, funding should not be an author's only contribution to the work.

Q: 5_Your article will appear in the following sections of the journal: Physical Sciences (Environmental Sciences) and Social Sciences (Sustainability Science). Please confirm that this is correct.

Q: 6_You have chosen not to pay an additional $1450 (or $1100 if your institution has a site license) for the PNAS open access option. Please confirm this is correct and note your approval in the margin.

Q: 7_Please verify that all callouts for supporting information (SI) citations in text are correct. Note, however, that the hyperlinks for SI callouts will not work until the article is published online. In addition, SI that is not composed in the main SI PDF (appendices, datasets, movies, and "Other Supporting Information Files") have not been changed from your originally submitted file and so are not included in this set of proofs. The proofs for any composed portion of your SI are included in this proof as subsequent pages following the last page of the main text. If you did not receive the proofs for your SI, please contact PNAS_Specialist.djs@sheridan.com.

Q: 8_Please check the order of your keywords and approve or reorder them as necessary. Note that PNAS allows up to five keywords; please do not add new keywords unless you wish to replace others.

Q: 9_Per PNAS style, certain compound terms are hyphenated when used as adjectives and unhyphenated when used as nouns. This style has been applied consistently throughout where (and if) applicable.

AUTHOR QUERIES

AUTHOR PLEASE ANSWER ALL QUERIES 2

Q: 10_Please confirm whether all units, divisions, departments, laboratories, or sections have been included in the affiliations line for each footnote symbol or add if missing. PNAS requires smallest institutional unit(s) to be listed for each author in each affiliation.

Q: 11_Please supply postal codes for affiliations a, b, c, d, and i.

Q: 12_PNAS does not allow claims of priority or primacy, hence the term “first” has been deleted.

Q: 13_If PCR-GLOBWB is an abbreviation, please spell out at first appearance and place the abbreviation in parentheses.

Q: 14_Please spell out ISI-MIP if it is an abbreviation.

Q: 15_Please note that italic font cannot be used for emphasis in text in PNAS.

Q: 16_Please verify that the phrases in quotes in sentence beginning "Beyond a correlation analysis" correspond to refs. 19 and 20, respectively.

Q: 17_PNAS does not allow claims of priority or primacy, hence the term “We are one of the first” has been deleted.

Q: 18_Please verify that "concentration" is meant as changed instead of "concertation."

Q: 19_Please clarify sentence beginning "We find that, although significant," particularly the first part.

Q: 20_Please define unit of measure “mma” here.

Q: 21_Fig. 4 is cited before Fig. 3. All figures must be cited in numeric order. Please correct.

Q: 22_Please note that Fig. S3 is cited out of order. Please modify the callouts to ensure that it is cited in numeric order.

Q: 23_Please verify insertion of the multiplication symbol after the expression "2.2–5.3" in sentence beginning "However, the absolute reductions." There was nothing after the numbers.

Q: 24_Please confirm edits to sentence “First, groundwater pumping likely decreases. . .”.

Q: 25_PNAS does not allow claims of priority or primacy, hence the term “novel” has been deleted. If the remaining sentence does not convey the intended meaning, please rewrite to avoid the claim of primacy but include citations of refs. 38 and 39.

Q: 26_PNAS articles should be accessible to a broad scientific audience. As such, please spell out "FAO" and delete the abbreviation, as it only appears once.

Q: 27_Please delete “in the research letter” if referring to this article. If not, please provide a reference and confirm that Fig. 1A is referring to a figure from a different publication.

Q: 28_Does "mm" stand for millimeters here, or for some other measurement?

Q: 29_Again, does Fig. 1B in the “research letter" refer to the present paper or a different paper?

AUTHOR QUERIES

AUTHOR PLEASE ANSWER ALL QUERIES 3

Q: 30_PNAS does not allow claims of priority or primacy, hence the term “new” has been deleted.

Q: 31_PNAS articles should be accessible to a broad scientific audience. As such, please spell out "FLUXNET." If a trade name, please indicate what type of drug/apparatus it is and the name of manufacturer.

Q: 32_Please note that “Eq. 1” under "Elasticity Calculations" has been changed to Eq. 4 to keep in chronological order.

Q: 33_Please verify that all et al. references contain 6 or more authors. If 5 authors or fewer, please supply complete author lists.

Q: 34_Please verify publisher location and supply page numbers for ref. 8.

Q: 35_Please supply page numbers for ref. 11. If the page numbers are identical to ref. 8’s page numbers, the references are duplicates and ref. 11 must be removed and the remaining references renumbered.

Q: 36_Is the report in ref. 14 published? If so, please supply publisher name and location. If not, it is an ephemeral reference and must be placed in a footnote. Also, please spell out COST.

Q: 37_Please supply publisher location and page numbers for ref. 20.

Q: 38_Please note that an asterisk at the end of the article title of ref. 23 has been deleted.

Q: 39_Please supply publisher location and page numbers for ref. 28.

Q: 40_Please supply volume number and verify accuracy of page numbers for ref. 37.

Q: 41_Please supply publisher location for ref. 43. If this is a program, please supply the version number.

Supporting Information

Hartmann et al. 10.1073/pnas.1614941114

Observed Recharge Rates

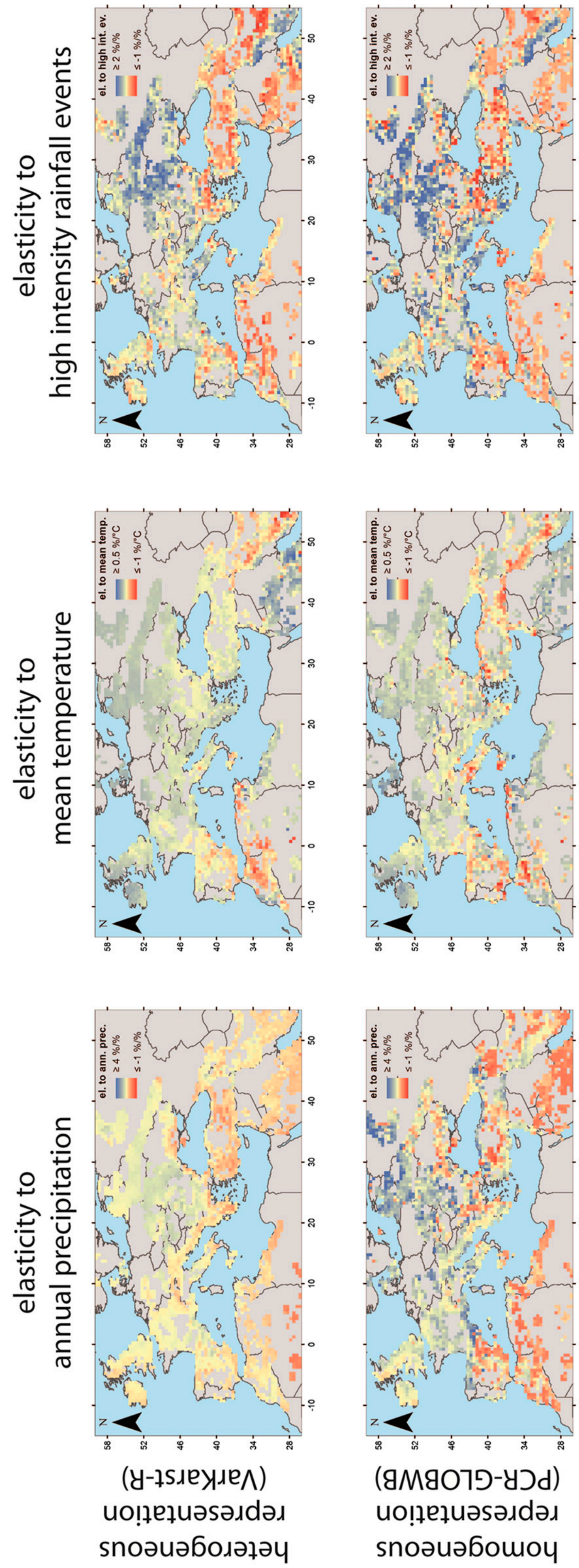

Fig. S1. Maps of derived recharge elasticities of the heterogeneous (*Top Row*) and homogeneous representation (*Bottom Row*) for the present period (1991–2010); color scale is set in accordance with the ranges chosen in Fig. 3 in the research letter.

Q:1

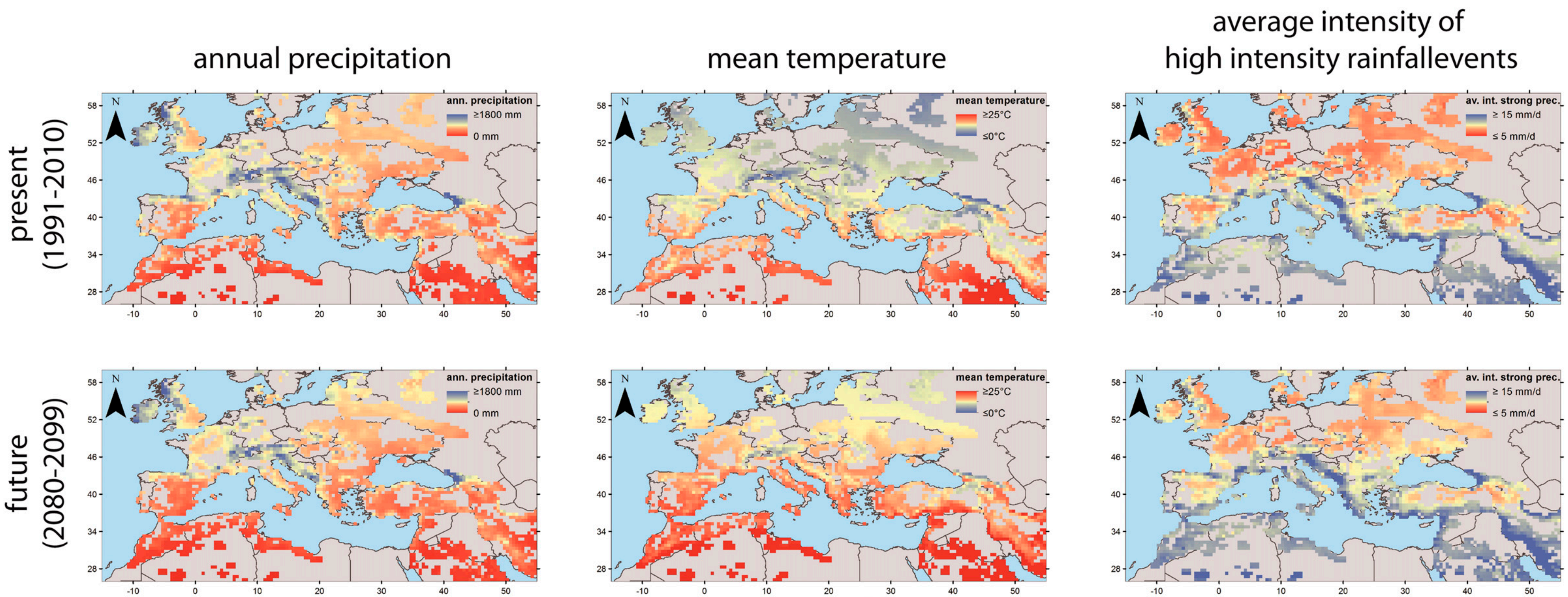

Fig. S2. Maps of precipitation, temperature, and mean intensity of high-intensity events for the present (1991–2010) and the future periods (2080–2099).

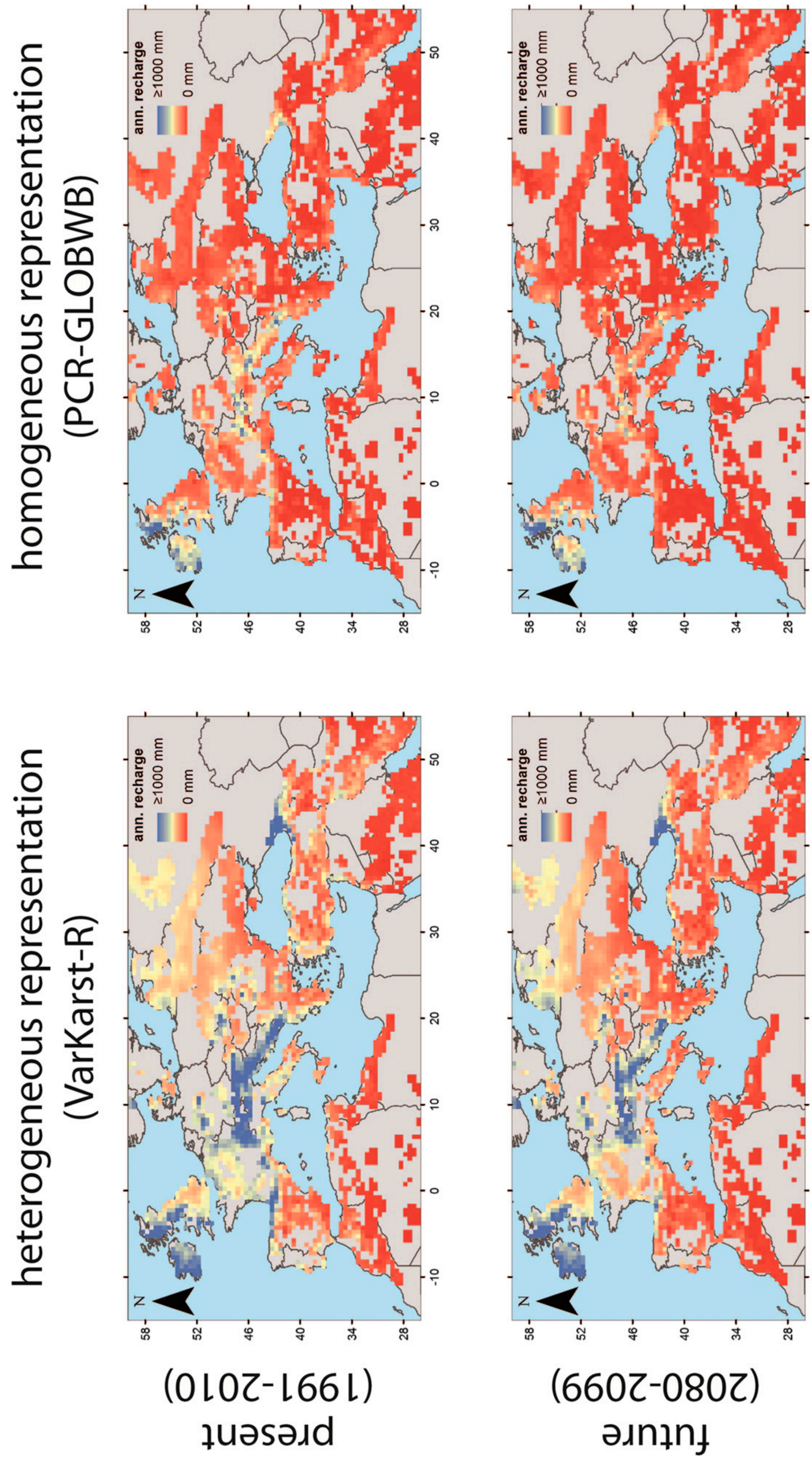

Fig. S3. Maps of simulated recharge rates by the heterogeneous and the homogeneous subsurface representations for the present (1991–2010) and the future periods (2080–2099).

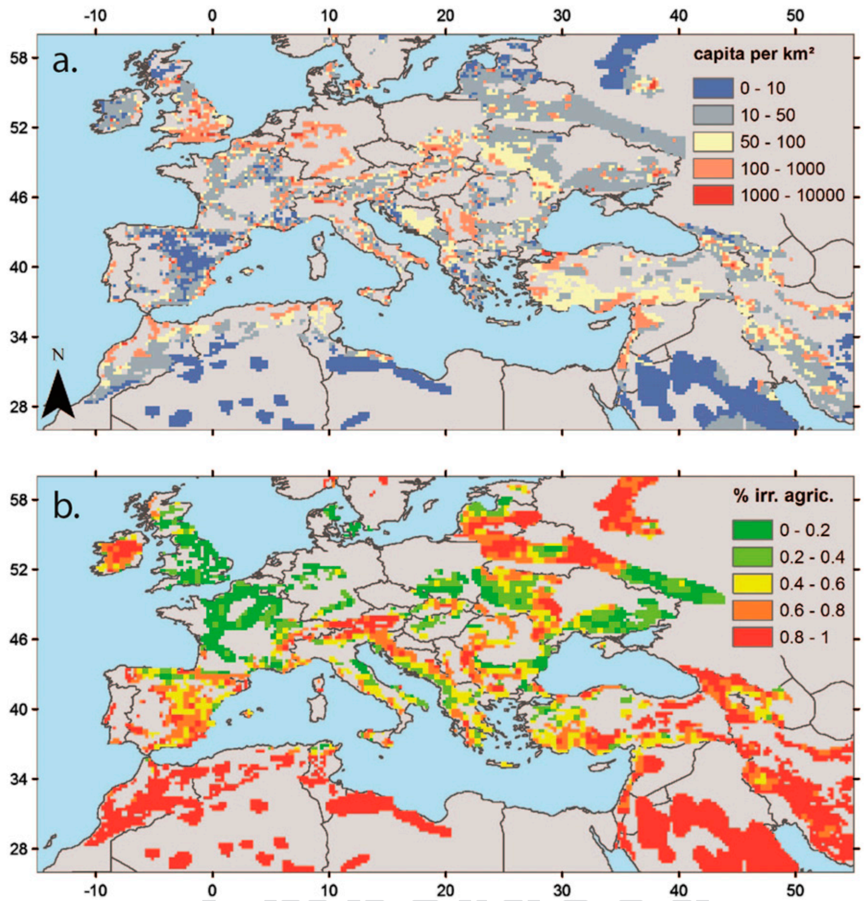

Q:2,3 **Fig. S4.** Population density (sedac.ciesin.columbia.edu/data/collection/gpw-v4) (*A*) and fraction of irrigated agriculture (edc2.usgs.gov/glcc/globe_int.php) (*B*) in Europe's and the Mediterranean's carbonate rock regions.

Table S1. Country, coordinates, mean annual recharge volumes, and reference of the 38 independent studies to evaluate the recharge simulation of the three models (see ref. 16 for list of references)

Country	Latitude, °	Longitude, °	Mean annual recharge, mm/a
Austria	47.69	15.6	686
Croatia	43.58	16.6	795
Croatia	45.22	13.6	385
France	45.8	0.44	250
France	44.01	3.16	378
France	43.92	5.13	566
France	43.93	3.85	213
Germany	48.93	11.3	130
Germany	48.21	9.15	350
Germany	49.2	11.8	200
Greece	35.13	24.55	241
Greece	38.6	21.15	484
Italy	41.88	12.9	416
Italy	41.05	14.55	559
Italy	42.27	13.34	700
Italy	40.78	15.13	973
Italy	39.9	15.81	693
Lebanon	33.73	35.93	333
Lebanon	34.08	36.3	205
Lebanon	34.05	35.95	841
Palestine	32	35.3	144
Portugal	37.1	−7.9	150
Portugal	37.1	−7.9	300
Saudi Arabia	26.5	46.5	44
Spain	37.9	−3.03	244
Spain	36.65	−5.72	318
Spain	36.93	−4.52	463
Switzerland	47.87	7.67	650
Turkey	36.97	33.22	552
Turkey	40.15	30.65	189
United Kingdom	51.53	−1.15	146
United Kingdom	51.53	−1.15	365
United Kingdom	50.75	−2.45	440
United Kingdom	52.6	0.88	260
United Kingdom	54.52	−1.87	690
United Kingdom	52.3	−2.58	355
United Kingdom	51.5	−1.53	234
United Kingdom	51.1	−1.26	348

AUTHOR QUERIES

AUTHOR PLEASE ANSWER ALL QUERIES

Q: 1_Does "research letter" refer to the main text of this paper? If so, please delete.

Q: 2_Please note that the URL in Fig. S4A legend (http://sedac.ciesin.columbia.edu/gpw) link redirects to http://sedac.ciesin.columbia.edu/data/collection/gpw-v4. Please confirm.

Q: 3_Please note that the URL in Fig. S4B legend (http://edc2.usgs.gov/glcc/globe_int.php) legend does not seem to work. Please correct.

Q: 4_Should mm/a in Table S1 be changed to mma for consistency?